*R. CAPUTO, **B. HELLY, ***S. PAVLIDES, ****G. PAPADOPOULOS,
*****O. TROJA, ***** A. GUELI

# PALAEOSEISMOLOGICAL TRENCHES ACROSS THE TYRNAVOS FAULT, CENTRAL GREECE

CONTENTS



ABSTRACT

The Tyrnavos Fault (TF) is an ESE-WNW trending, north-dipping dip-slip normal fault representing one of the major tectonic structures bordering the Late Pleistocene-Holocene Tyrnavos Basin, Northern Thessaly, Greece. The fault affects Quaternary and Pliocene deposits and mainly the Triassic crystalline limestone of the Pelagonian basement. According to previous researches, the TF has been clearly geometrically and kinematically characterised. A well-defined fault trace has been mapped for more than 12 km, while remote sensing techniques allow to follow it further East across the northern Larissa Plain, thus giving a possible total length of almost 20 km.

In this note, the results of a palaeoseismological investigation carried out along the fault will be presented and discussed.

KEY WORDS: Seismic hazard, seismotectonics, morphogenic earthquakes, Aegean, Holocene.

## 1. INTRODUCTION

Since a decade, the Tyrnavos Fault has been characterised as an active fault mainly based on geological, structural and morphological evidences (CAPUTO, 1990; 1993b) as well as geophysical investigations (CAPUTO & HELLY, 2000; CAPUTO *et alii*, 2003). On the other hand, only few historical earthquakes occurred within the broader area of northeastern Thessaly and no events have been documented to be directly associated to this structure. This research is devoted to investigate past morphogenic earthquakes (*sensu* CAPUTO, 1993a) following a palaeoseismological approach.

The investigated site has been selected along the eastern sector of the Tyrnavos Fault where a linear morphological scarp has been recognised along the southern slope of an E-W trending valley, near locality Fardolakka, about 5 km SSW of Tyrnavos town (Fig. 1). This morphological feature has been associated to the cumulative effects of repeated seismic events (CAPUTO, 1993b). According to geological mapping, the footwall block is characterised by Late Quaternary alluvial-colluvial sediments resting in paraconformity on Pliocene carbonate deposits that partly overlap the Triassic limestone with a strong angular unconformity. In contrast, the hanging-wall block is covered by Late Pleistocene-Holocene alluvial-colluvial materials and detrital deposits of local origin (Fig. 1b).

At this site, we excavated three palaeoseismological trenches (Fig. 1b). Two of them are located across the well defined shear zone between the bedrock of the footwall block, here consisting of Pliocene limestone, and the loose late Quaternary deposits of the hanging-wall block, while the third one is mainly located within the footwall block and partly crosses a smooth morphologcal scarp within the alluvial plain where the fault trace spreads out. This trench distribution also allowed us to observe the along strike variability in morphogenic behaviour of an active fault.

## 2. PALAEOSEISMOLOGICAL TRENCHES

### 2.1. *Trench A*

This is the westernmost trench and it is oriented N-S, orthogonal to the local trend of the fault trace (Fig. 1a) here represented by more than one-meter high morphotectonic scarp. In the footwall block, Pliocene-Early Pleistocene limestone crop out consisting of subhorizontal oolitic calcarenites, in medium to thick layers that are locally welded together. These deposits were probably formed as beachrocks along the palaeo-coast of the Villafranchian Thessalian lake (CAPUTO, 1990). The two trench walls (Fig. 2) are nearly 3 m apart and about 10 m long. The trench cross cuts the contact zone and it has been excavated 2-3 m within the bedrock of the footwall block, locally softened and parted by intense vertical fracturing. Close to the contact plane, fractures are well developed, well connected and certainly extending much deeper. Indeed, at about 3 m depth from the top surface, fractures in the limestones are open up to several centimetres and from one of these features cool air blows out during the hot summer of Thessaly thus documenting underground circulation.

In the hanging-wall block, alluvial and colluvial deposits are observed. Due to the proximity of the source rocks and the simple geology of the footwall block, the composition of all the detrital clasts is fairly uniform. Clasts are from millimetres to decimetres in size and generally

* Di.S.G.G., University of Basilicata, Potenza, Italy. E-mail. rcaputo@unibas.it
** Maison de l'Orient Méditerranéen Jean-Pouilloux, Lyon, France.
*** Dept. of Geology, Aristotle University of Thessaloniki, Thessaloniki, Greece.
**** National Observatory of Athens, Athens, Greece.
***** Dept. of Physics, University of Catania, Catania, Italy.

a)

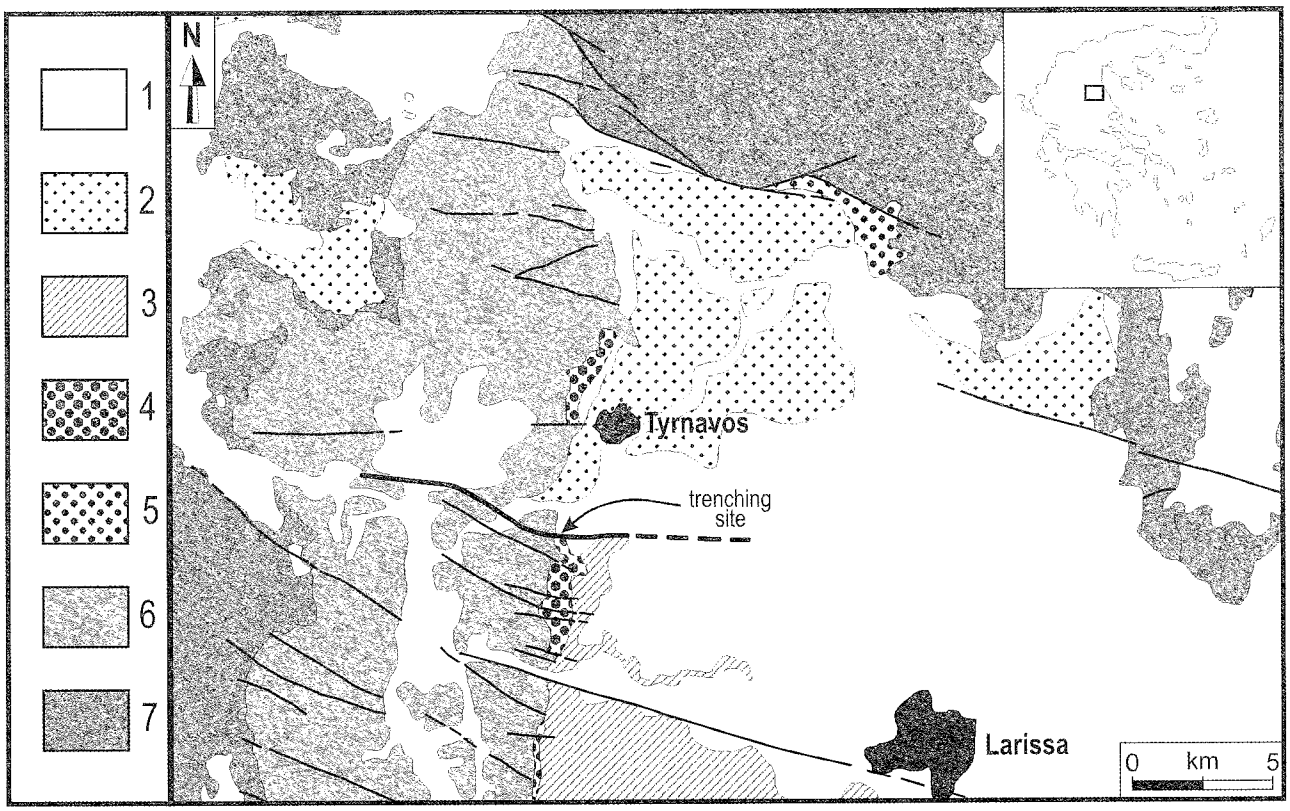


b)

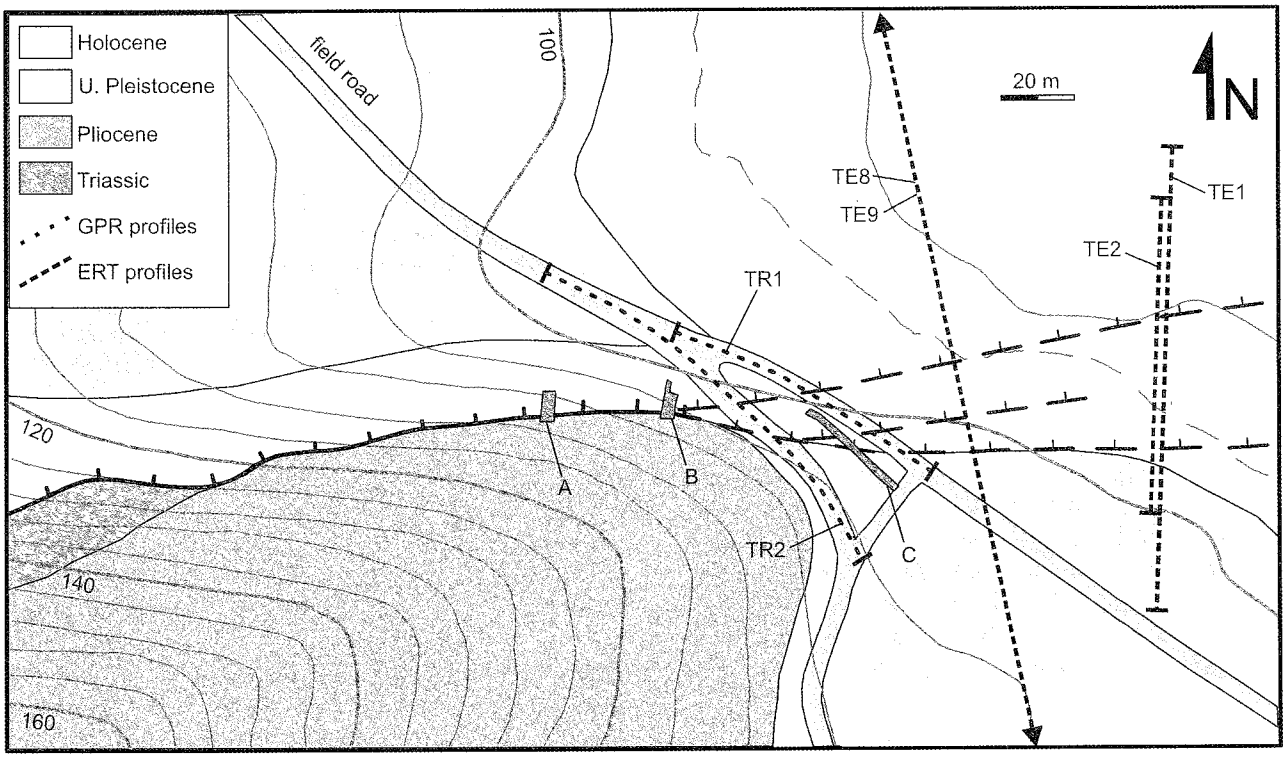


Fig. 1 - a) Simplified geological map of eastern Thessaly. 1: Holocene deposits; 2: Villafranchian; 3: Pliocene fluvio-lacustrine; 4: Tyrnavos Fm (Pliocene?); 5: Rodia Fm (Pliocene?); 6: Triassic limestone; 7: undifferentiated bedrock. Inset map for location. b) Geological and structural map of the investigated site with the location of the excavated palaeoseismological trenches.

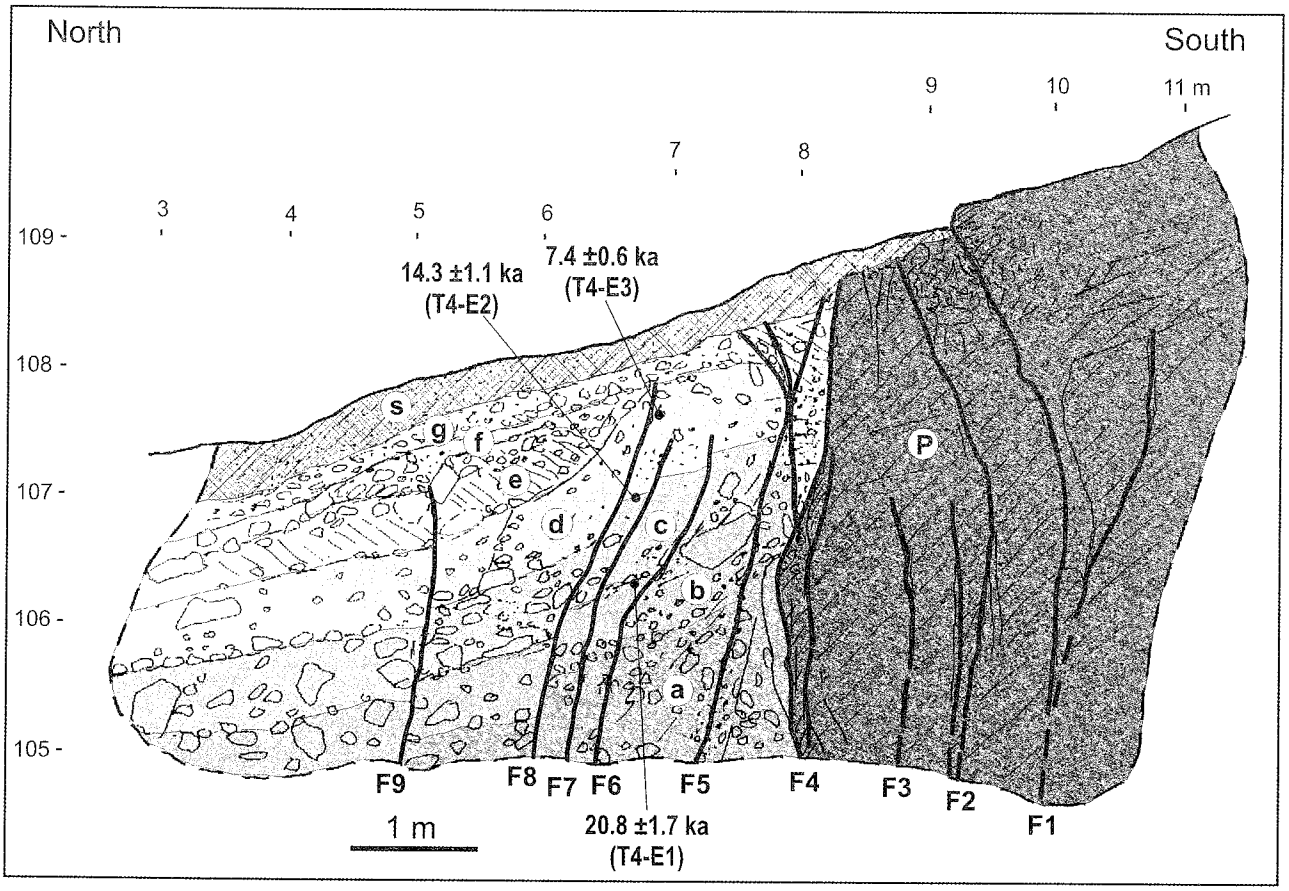


Fig. 2 - Log of the eastern wall of trench A excavated across the tectonic contact between the Pliocene-Lower Pleistocene carbonate and the latest Pleistocene-Holocene eluvial and colluvial deposits. Letters within white circles refer to sedimentary units while faults are numbered (F#). Location and age of samples are also reported (see Tab. 1 for details).

subangular to angular in shape. Matrix is commonly abundant and only locally the texture is clast-supported. Slight variations of the matrix colour, of the size and distribution of clasts, some incipient pedogenesis on top of the strata and a locally observed fining upwards gradation allow to distinguish the layering and to separate at least 7 sedimentary units (labelled *a* to *g*). All layers are dipping north by about 15°-20° and their thickness ranges from 25 to 80 cm, locally showing a wedge-shape geometry.

The above described sedimetary succession is covered by an incipient brown soil (labelled *s*) consisting of organic-rich fine-grained material with scattered subangular carbonate clasts.

The entire succession, with the exception of the soil layer, is affected by several fracture planes that show variable displacements from few centimetres up to 50 cm each (faults *F5* to *F9*). Accordingly, the cumulative vertical displacement of the lowermost sedimentary layer (labelled *a*) caused by these faults is more than one metre. However, if we also consider the displacement associated to the principal fault plane separating the bedrock from the Quaternary sediments (labelled *F4*) the total amount of shear between the two blocks is larger than 3.5 m. Minor fractures with some synthetic displacement have been also observed within the Pliocene limestone of the footwall block.

### 2.2. *Trench B*

Trench B has been excavated nearly N-S (N10°E), but not perfectly orthogonal to the local trend of the fault trace, which here is oriented N80°E (Fig. 1b). The trace is here emphasised by a morphological scarp similar to that observed in correspondence of trench A, though fairly more weathered. Also in this case the trench (Fig. 3) is nearly 3 m wide and the excavation is about 10 m long. Again, the bedrock of the footwall block consists of Pliocene-Early Pleistocene oolitic calcarenites dipping about 10° to the south. Fracturing within the bedrock is here less intense than in trench A and consequently the medium to thick layering is more evident than in the former case. On the other hand, the contact zone observed in trench B is much more clear and sharp than in A and dips about 75° to 80° northwards. Indeed, the cataclastic process is much more localised and thus more intense. As a consequence, the mechanical process of fracturing has generated a real breccia layer generally fine-grained and with relatively abundant matrix (labelled $k_1$). The cataclastic material is characterised by the isorientation of the long axis of the irregularly shaped clasts. Especially in the deepest sector of the trench, a well defined cleavage can be observed, consisting of numerous shortly spaced shear

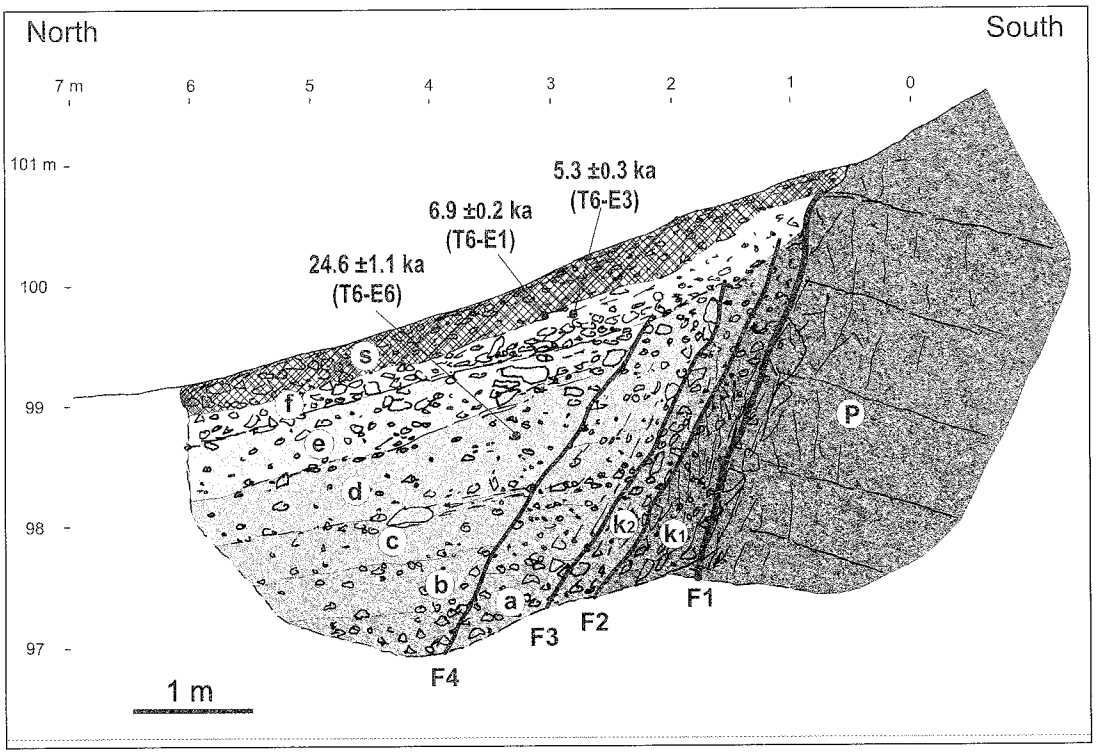


Fig. 3 - Log of the eastern wall of trench B excavated across the tectonic contact between Pliocene-Lower Pleistocene carbonate rocks and the latest Pleistocene-Holocene eluvial and colluvial deposits. Symbols as in figure 2.

planes oriented either parallel to the main contact surface as well as subvertical. These latter features are interpreted as Riedel structures synthetic with the normal dip-slip displacement occurring along the fault. The thickness of the fault gouge is about 80-100 cm at 3 m depth and it progressively thins upwards till disappearing near the surface. However, a zone of evident tectonic perturbation, showing a partial obliteration of the layering and the occurrence of minor fracture planes parallel to the contact surface, is certainly wider and almost double and is represented as $k_2$ zone in figure 5.

The materials belonging to the hanging-wall block consist of organised clastic deposits dipping about 15°-20° to the north. The origin and consequently the lithology of the clasts is the same as in trench A. Particles are from millimetres to few decimetres in size and subangular to angular in shape. Layers show more clearly a fining upwards gradation (labelled *a* to *f*). Texture is commonly matrix-supported though locally the coarse-grained lower portion of the layers is clast-supported. The clay-silty matrix is yellowish to light brown in colour. Single strata have a thickness ranging from 25 to 80 cm, while a slight thickening seems to occur toward the shear zone (*viz.* wedge shape). The typical organic-rich brown soil (labelled *s*) blankets the alluvial and colluvial succession.

As above mentioned, in trench B the slip is concentrated within a relatively narrow shear zone (labelled $k_1$ and $k_2$) defined by faults *F1* to *F3*, in figure 3. Only one minor fault (labelled *F4*) has been observed outside this zone. The minimum amount of total displacement for the lowermost sedimentary layer (labelled *a*) is about 4 m that is comparable with that observed in trench A.

### 2.3. *Trench C*

Trench C has been entirely excavated within the alluvial deposits across the southern sector of a smooth morphotectonic escarpment existing east of the major fault trace that affects the bedrock (Fig. 1b). Ground Penetrating Radar profiles parallel to this trench show several ruptures and cumulative dislocations of the dielectric horizons at very shallow depth (CAPUTO & HELLY, 2000). The trench is 36 m long, 2 m wide and 3 to 3.5 m deep with a N50°W strike.

From the detailed log of the trench walls (Fig. 4) only few layers can be recognised (*a* to *c*). From the bottom we distinguished a 1.2-1.6 m thick layer of yellowish-reddish sandy silt with a variable amount of clay content (unit *a*). Whitish carbonate-rich patches are frequent within these materials, locally resembling a sub-horizontal but discontinuous layering. At places, real carbonate nodules have been observed. Clasts from millimetres up to few centimetres are rare. This unit could represent the B-horizon of a calcic soil, though local concentrations of this carbonate material could have been enhanced by the co-seismic fracturing process (faults *F1* to *F4*).

On top of this silty layer there is an alluvial deposit consisting of subangular to subrounded clasts from millimetres to few decimetres in size and with abundant reddish-brown mainly muddy-silty matrix (unit *b*). In this trench, the clastic alluvial bed is slightly thicker varying

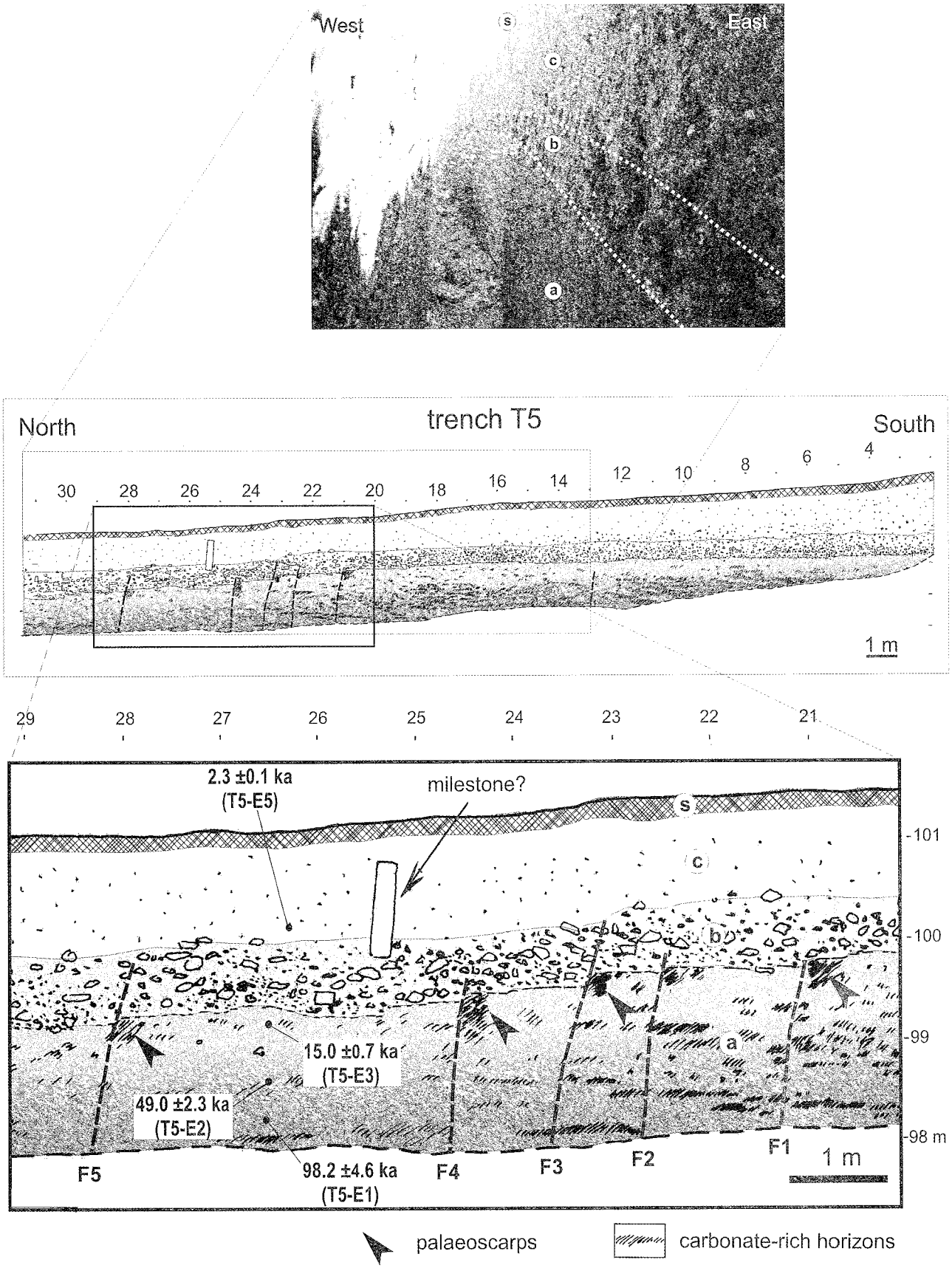


Fig. 4 - The western wall of trench C excavated across the smooth morphological escarpment. (top) Internal view. (centre) The log of the western wall. (bottom) Detail of the northern sector of the trench. Note the occurrence of several ruptures associated to small dislocations of the alluvial bed and to anomalous concentrations of whitish carbonate cement. During the excavation we found an almost 1 m high squared stone vertically posed, which probably represents a milestone. Symbols as in figure 2.

from 40 to 60 cm. Unit *b* is overlain by a layer of yellowish to light brown sand and silt with some clay content (unit *c*). It contains scattered small clasts and it does not show any particular internal sedimentary structure. The thickness is about 1 m. The trench wall is capped by the typical active brown soil about 10 cm thick (unit *s*).

## 3. DISCUSSION

In order to better specify the seismic periods and to date single past earthquakes, several samples have been collected from the three trenches. The samples were dated with different techniques (see Table 1) and specifically with thermo-luminescence (TL), optically stimulated luminescence (OSL) and accelerated mass spectrography (AMS). All samples consist of sandy-silty sediments, except one sample being the shell of a continental Mollusc. Further details for each sample are listed in table 1.

Based on the similarities of the stratigraphic successions observed in trenches A and B, we attempted a palinspastic restoration. In figure 5, each sketch represents an interseismic period and obviously between each 'photogram' at least one morphogenic earthquake occurred (events 1 to 8). In both trenches, the chronologies are consistent with, and clearly confirm, a latest Pleistocene to Holocene age of the deposits affected by the Tyrnavos Fault. However, although if we take into account the high lateral variability of this kind of continental deposits, the absolute ages of the two stratigraphic successions partially disagree at depth. In particular, layer *b* in trench A has been dated 20.8 ±1.7 ka while layer *d* in trench B has been dated 24.6 ±1.1 ka, but it is important to note that samples from trench A have been analysed with the TL technique, while from trench B, OSL and AMS techniques have been used. At this regard, recent researches have emphasised that the sunlight is insufficient to generate a complete TL resetting in the crystals (POOLTON & ROBERTSON, 1997). Consequently, the use of the TL technique has strong limitations for dating sediments and it has been progressively superseded by the OSL technique. Accordingly, we tentatively base the chronology of our palaeoseismological interpretation on the samples from trench B.

Our attempt in dating single earthquakes faces two further problems. Firstly, the long-term sedimentation rates that we can obtain from the analysis of trenches A and B are about 0.1-0.05 mm/a. As a consequence of these relatively low rates, sedimentation is highly condensed. Secondly, due to the sub-aerial conditions of the investigated site, a slow sedimentation rate also implies the occurrence of deeply working weathering phenomena and of pedogenic processes along with a more or less intense biological amalgamation of the whole uppermost section of the layer. Consequently, due to the condensation and the natural mixing of the sediments, the sampling operations become somehow problematic, but above all the interpretation of the obtained sample ages must be attentive.

Based on the available dates we can constrain the possible time windows of past earthquakes. The most recent event (event 1) occurred between Present and 5.3-6.9 ka BP and caused the accommodation space for the soil layer *s* of about 10-20 cm (Fig. 5). It is noteworthy to mention that west of the trenching site, along the fault trace, an almost unweathered strip of bedrock, relatively uniform in height and ranging between 5 and 15 cm, can be followed for several hundreds of meters as documented by CAPUTO (1993b). This surficial feature, which has been interpreted as a *morphogenetic* effect (*viz.* free face), is possibly related to event 1.

The penultimate earthquake (event 2) possibly occurred in the same time window (Present to 5.3 ka BP) and was associated to 20-30 cm (Fig. 5). Event 3 occurred before 5.3-6.9 ka BP (and much after 24.6 ka BP) showing a vertical displacement of about 20-25 cm in both trenches.

In the same time window (6.9 to 24.6 ka BP), but

| trench | sample | material | unit | age (ka) BP | error (± ka) | method | lab. | lab# |
|---|---|---|---|---|---|---|---|---|
| A | T4-E1 | se | b | 20.8 | 1.7 | TL | BJ | T4W-1 |
| | T4-E2 | se | c | 14.3 | 1.1 | TL | BJ | T4W-2 |
| | T4-E3 | se | d | 7.4 | 0.6 | TL | BJ | T4W-3 |
| C | T5-E1 | se | a | 98.2 | 4.6 | OSL | CT | t5e1 |
| | T5-E2 | se | a | 49.0 | 2.3 | OSL | CT | t5e2 |
| | T5-E3 | se | a | 15.0 | 0.7 | OSL | CT | t5e3 |
| | T5-E5 | se | c | 2.3 | 0.1 | OSL | CT | t5e5 |
| B | T6-E1 | sh | f | 6.9 | 0.2 | AMS | UGA | 10360 |
| | T6-E3 | se | f | 5.3 | 0.3 | OSL | CT | t6e3 |
| | T6-E6 | se | d | 24.6 | 1.1 | OSL | CT | t6e6 |

Tab. 1 - Samples collected from palaeoseismological trenches and relative ages in ka BP. *Sample*: label used in the present note; *material*: se = sediment; sh = shell; *unit*: letters refer to sedimentary units as labelled in the figures corresponding to each trench (Figs. 5 to 8); *method*: TL = thermoluminescence; OSL = optically stimulated luminescence; AMS = accelerated mass spectrography; *lab.*: CT = Department of Physics, University of Catania, Italy (resp. O. Troja); UGA = Center for Applied Isotope Studies, University of Georgia, Athens, USA (resp. R. Culp); BJ = Institute of Geology, State Seismological Bureau, Beijing, China (resp. C. Shaoping); *lab#*: sample label used in the laboratory.

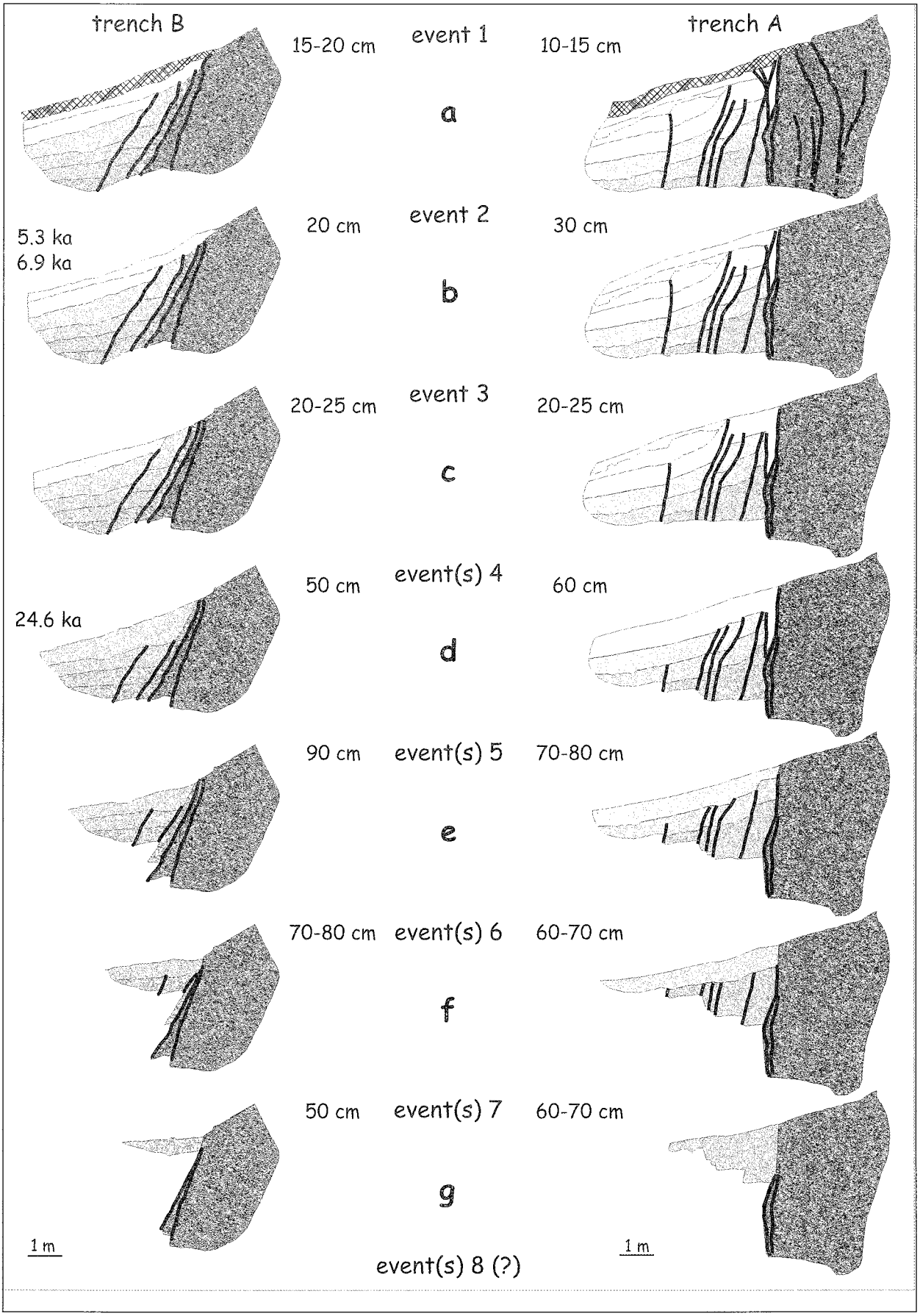


Fig. 5 - Palinspastic restoration of trenches A and B. The different sketches correspond to the interseismic periods. At least one seismic event occurred between two successive sketches. For each seismic event(s) the vertical displacement is also represented for the two trenches.

probably much closer to 24.6 ka BP, a further earthquake affected this fault sector (event 4). Eventually, events 5 to 8 show vertical displacements between 50 and 90 cm, comparable in the two trenches, that certainly occurred before 24.6 ka BP though the lower time boundary is open.

In order to estimate the amount of co-seismic dislocation, we followed a straightforward geometric restoration for each seismic event. The obtained values are reported in figure 5. As we can see, the amount of vertical displacement observed in the two trenches agree quite well especially if we take into account the nature of the involved sediments.

According to the relationships between the maximum vertical displacement and the magnitude of a morphogenic earthquake proposed by PAVLIDES & CAPUTO (2003), the 10 to 90 cm of superficial fault slip correspond to M=6.3 to M=6.7, respectively (±0.1 for the 95% confidence interval). However, a magnitude of 6.7 ±0.1 should correspond to a surface rupture length of more than 20-25 km (PAVLIDES & CAPUTO, 2003) and this inference poses two major problems. Firstly, the total length of the Tyrnavos Fault directly mapped in the field is about 12 km (CAPUTO, 1993b), though based on remote sensing analyses the fault seems to continue eastwards across the Larissa alluvial plain up to a possible maximum length of 20 km. Secondly, as a consequence of a morphogenic earthquake, the maximum vertical displacement commonly occurs within the central sector of the seismogenic structure, while our trenching site is located in a lateral sector. Accordingly, it is likely that the vertical displacements observed in the palaeoseismological trenches larger than 30-40 cm (events 4 to 7, in Fig. 5) are the cumulative result of at least two distinct events. As above mentioned, the condensed sedimentation and the continental character of the excavated deposits certainly do not make easier the stratigraphic interpretation and confident the separation of the single layers.

As concerns trench C, the obtained absolute ages show a stratigraphic sequence highly condensed with respect to the other two trenches (2.5 m in about 100 ka). This is due to the fact that this trench is mainly located within the footwall block and therefore this sector of the plain was not affected by co-seismic subsidence. On the other hand, the set of fractures and the slight warping of the sedimentary succession indicate that deformation within these soft sediments of the alluvial plain was limited, diffuse and it is not concentrated as it occurs along the bedrock-sediments contact (trenches A and B). Based also on the results of the geophysical investigations carried out within the same area, the lateral variability in morphogenic behaviour of this active fault is highlithed showing the upwards branching and the general partitioning of the co-seismic deformation process when affecting loose or poorly consolidated deposits in contrast to occurs across the bedrock.

## 4. CONCLUDING REMARKS

The palaeoseismological trenches substantiate the Late Pleistocene to Holocene morphogenic activity of the Tyrnavos Fault as previously inferred from morphotectonic (CAPUTO, 1993b) and geophysical (CAPUTO & HELLY, 2000; CAPUTO et al., 2003) investigations. The seismotectonic evolution of the Tyrnavos Fault as inferred from the palaeoseismological trenches is characterised by numerous morphogenic earthquakes during latest Pleistocene-Holocene times. According to the available data, the recurrence interval for major earthquakes capable of producing some tens of centimetres of vertical displacement along this sector of the fault is in the range of some thousands of years, say 2 to 4 ka. However, following the same line of reasoning forced by the problems of the stratigraphic interpretation, a possible alternative scenario consists of a larger number of morphogenic earthquakes, each one generating 10-30 cm of vertical displacement and consequently with a shorter return period, say 1.5-3 ka.

According to the magnitude versus displacement empirical relationships (PAVLIDES & CAPUTO, 2004), the two palaeoseismological scenarios obviously imply important differences in the amount of released co-seismic energy. In fact, in the former case earthquakes have likely magnitudes as high as 6.6-6.7, while in the latter case, more frequent earthquakes have magnitudes probably ranging between 6.2 and 6.4. Any estimate of the seismic hazard assessment relative to the Tyrnavos Fault and the whole northern Larissa Plain will be strongly influenced by the selected model.

In our opinion and according to preliminary results obtained from other palaeoseismological trenches excavated along the central segment of the Tyrnavos Fault and comparing the presented data with those obtained in other palaeoseismological investigations carried out along similar Aegean-type (Pavlides and Caputo, 2004) normal faults (Pavlides, 1996; Chatzipetros et al., 1998), the second proposed scenario seems to be more likely.

## REFERENCES


CAPUTO R. (1990) - *Geological and structural study of the recent and active brittle deformation of the Neogene-Quaternary basins of Thessaly (Greece).* Scientific Annals, **12**, Aristotle University of Thessaloniki, **2/5**, 252 pp., Thessaloniki

CAPUTO R. (1993a) - *Morphogenic earthquakes: a proposition.* Bull. INQUA-Neotectonic Comm., **16**, 24, Stockholm.

CAPUTO R. (1993b) - *Morphotectonics and kinematics along the Tirnavos Fault, northern Larissa Plain, mainland Greece.* Zeit. fur Geomorph., **94**, 167-185.

CAPUTO R. & HELLY B. (2000) - *Archéosismicité de l'Égée: étude des failles actives de la Thessalie.* Bull. Correspondance Hellenique, **124**, 2, 560-588, Athens.

CAPUTO R., PISCITELLI S., OLIVETO A., RIZZO E. & LAPENNA V. (2003) - *The use of electrical resistivity tomography in Active Tectonic. Examples from the Tyrnavos Basin,* Greece. J. Geodyn., **36**, 1-2, 19-35.

PAVLIDES S. & CAPUTO R. (2004) - *Magnitude versus faults' surface parameters: quantitative relationships from the Aegean.* Tectonophysics, **380**, .

POOLTON N.R.J. & ROBERTSON G.B. (1997) - *Sediment dating by luminescence.* Radiation Measurement, **27**, 893-922.